Matched-field processing, geoacoustic inversion, and source signature recovery of blue whale vocalizations

Aaron M. Thode, G. L. D'Spain, and W. A. Kuperman
Marine Physical Laboratory, Scripps Institution of Oceanography, San Diego, California 92093-0205

(Received 28 December 1998; revised 25 October 1999; accepted 27 October 1999)

Matched-field processing (MFP) and global inversion techniques have been applied to vocalizations from four whales recorded on a 48-element tilted vertical array off the Channel Islands in 1996. Global inversions from selected whale calls using as few as eight elements extracted information about the surrounding ocean bottom composition, array shape, and the animal's position. These inversion results were then used to conduct straightforward MFP on other calls. The sediment sound-speed inversion estimates are consistent with those derived from sediment samples collected in the area. In general, most animals swam from the east to west, but one animal remained within ~500 m of its original position over 45 min. All whales vocalized between 10 and 40 m depth. Three acoustic sequences are discussed in detail: the first illustrating a match between an acoustic track and visual sighting, the second tracking two whales to ranges out to 8 km, and the final sequence demonstrating high-resolution dive profiles from an animal that changed its course to avoid the research platform FLIP (floating instrument platform). This last whale displayed an unusual diversity of signals that include three strong frequency-modulated (FM) downsweeps which contain possible signs of an internal resonance. The arrival of this same whale coincided with a sudden change in oceanographic conditions.
[S0001-4966(00)02802-2]

PACS numbers: 43.30.Pc, 43.30.Sf [WA]

INTRODUCTION AND REVIEW OF PREVIOUS WORK

In this paper, matched-field processing[1–3] (MFP) methods have been applied to blue whale (*Balaenoptera musculus*) vocalizations, recorded off the California coast in 1996. The research upon which this work is based is an outgrowth of initial work by the Marine Physical Laboratory to conduct MFP on whales during an unrelated experiment in 1994,[4,5] and to use whale vocalizations for geophysical inversions.[6] The results presented in this paper show how these techniques can obtain high-resolution ranges and depths of blue whale positions out to ranges of 8 km under complex propagation conditions, using as few as eight hydrophones. No previous knowledge of the surrounding ocean bottom was required, because the needed information was extracted from the vocalizations themselves, using global inversion techniques. When combined with the acoustic vector intensity measured from a DIFAR[7] sonobuoy, a three-dimensional localization was achieved. Propagation effects could then be removed from the calls, using the derived locations and inferred ocean bottom properties. This procedure obtained estimates of both the source time signatures and source levels of different vocalization types.

Most localization work on baleen whales has focused on obtaining azimuth and range, usually by employing widely spaced hydrophone assemblies. Recent examples of these approaches are given in Refs. 8–11. Previous depth estimates from cetacean vocalizations have been obtained only under restricted conditions, where the acoustic signal has been assumed to travel directly from the animal to each receiver, allowing standard time-of-arrival methods[12] to be employed. Some examples of this approach have included captive dolphins in a concrete tank,[13] and sperm whales in deep water.[14] However, acoustic signals generated by baleen whales along the coast generally propagate over ranges greater than the local water depth, and they become substantially altered through interaction with the surface and ocean bottom, making the application of standard time-of-arrival methods difficult.[12] The MFP techniques used in this paper have no such limitations; indeed, some signals discussed here have been localized in depth and range to distances greater than 60 times the local water depth, and thus experienced multiple surface reflections and bottom refractions before being recorded. In this case no direct acoustic path between the whale and the receiving array existed.

After a review of the experimental location, geometry, and data analysis procedures in Sec. I, the MFP results are presented in Sec. II A, using data from three distinct acoustic sequences, recorded over a 40-hour time period in 1996 off the northern Channel Islands in the Southern California Bight region. The first sequence (case 1) demonstrates a match between an acoustic track and a visual observation of two blue whales. The next sequence (case 2) demonstrates the maximum ranges obtained from the experiment, covering a 90-min period wherein two different whales are tracked to ranges of several kilometers. The final sequence (case 3) illustrates a high-resolution track of a single whale that swam toward the research platform FLIP, then altered its course to avoid the experiment. This sequence contains three unusual FM signals and three detailed dive profiles.

Section II B compares the sediment properties extracted from the whale vocalizations with those derived from sediment cores taken from the same region. Section II C uses the MFP positions to compute source levels for the animals in cases 2 and 3, and Sec. III D uses multichannel deconvolution techniques[15,16] to strip away propagation effects from three FM sweeps in case 3, demonstrating that the unusual

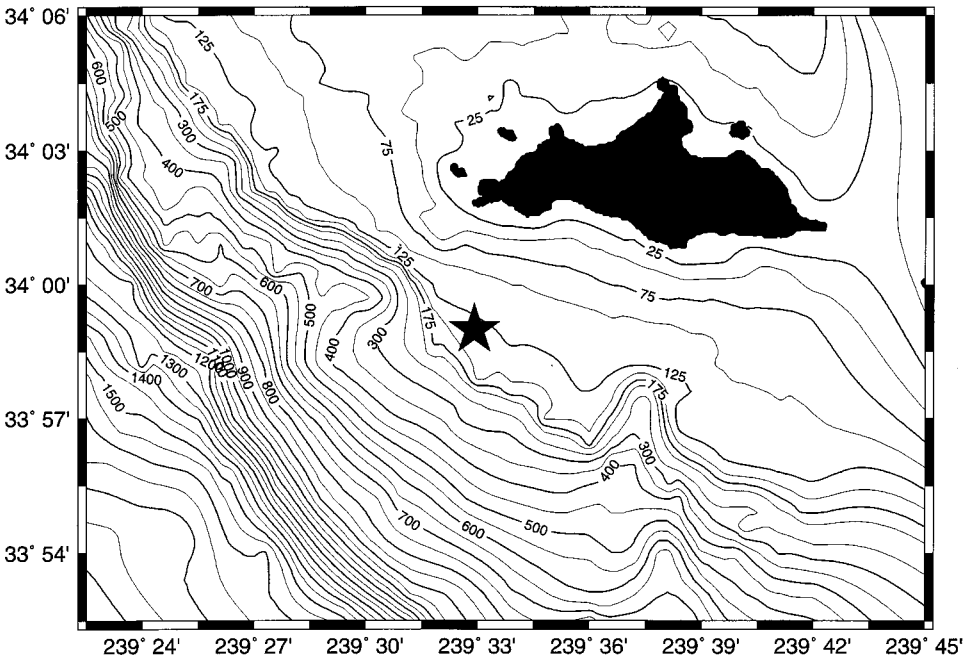

FIG. 1. Bathymetry around the 1996 experiment site. The contour interval is 25 m until 300-m depth, and then increases to 50 m for deeper depths. FLIP location is given by star. Note how the bathymetry to the east and northwest is only mildly range-dependent.

features present in the call are produced within the whale itself, and are not waveguide effects. The discussion in Sec. III discusses whether the unusual FM sweeps in the latter case might indicate an internal resonance, and notes how the presence of this whale coincides with a sudden change in ocean conditions in the area.

The ''type A'' and ''type B'' eastern Pacific blue whale vocalizations discussed here are described in greater detail elsewhere.[8–10,17,18] References on blue whale sounds in other regions of the world,[19–25] MFP,[1,2,26,27] and geoacoustic inversion methods,[26,28–34] have also been provided.

I. METHODS

A. Experiment location and geometry

The 1996 experiment was conducted using the research platform FLIP (floating instrument platform)[35] from July 18 through July 22 off the south coast of San Miguel Island, at 33°59′ N, 120°27.221′ W. This location lies within the boundaries of the Channel Islands National Marine Sanctuary,[36] administered by the National Oceanic and Atmospheric Administration. Surveys over the past ten years have observed concentrations of blue, fin, and humpback whales in the region during the summer months. ''Whale Habitat and Prey Study (WHAPS)'' surveys[37] conducted by the National Marine Fisheries Service, Southwest Fisheries Science Center (SWFSC) have concluded that around 100 blue whales frequent the area each summer. The animals are believed to be feeding off krill, which in turn feed off the plankton blooms growing in the nutrient-rich water upwelling around the islands.[38]

Figure 1 illustrates the bathymetry around the experimental site. The contour maps were constructed using fathometer-corrected data downloaded from the National Oceanographic Service and National Geological Data Center databases. Depending on the tide level, the water depth at the experiment site varied between 129 and 133 m. The vocalizations presented here will be from animals swimming from the E to SE of FLIP, a region where the water depth changes by only 30 m over 10 km.

The experimental deployment is illustrated in Fig. 2, and consisted of a 48-element[39] vertical array with a hydrophone spacing of 1.875 m, sampled at a rate of 1500 Hz. A General Oceanics inclinometer was attached 1.7 m above the shallowest hydrophone element, and recorded the array tilt magnitude and direction, inclinometer depth, and water temperature every 90 sec. Data from the vertical array were used to conduct the MFP, while information from both the vertical array tilt and an occasional DIFAR sonobuoy[7] estimated

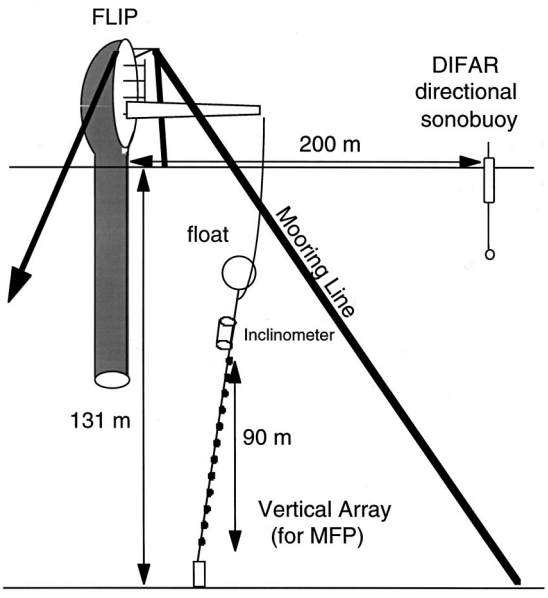

FIG. 2. Experimental setup of the MFP experiment. The vertical array is used to compute range and depth of calling animals. Source azimuth could occasionally be estimated by using either a DIFAR directional sonobuoy (as in case 2), or by taking advantage of the vertical array tilt caused by strong currents in the area (Sec. I C). The thick dark lines represent mooring lines.

source azimuth,[40,41] thus yielding a three-dimensional location. Subsequent work showed that localization could be accomplished using as few as eight hydrophones as long as they spanned 90 m of vertical aperture.

B. Data analysis and inversion procedures

Traditional MFP requires information about the ocean depth, bottom composition, sound-speed profile, and tilt of the vertical array, in order to construct an accurate model of the acoustic field received at the area. Bathymetry information was independently available, but the other environmental information was sparse or unknown. The analysis for each case presented in Sec. II began by selecting several large signal-to-noise ratio (SNR) calls throughout the sequence for ''focalization'' or inversion. By applying a genetic algorithm[42,43] inversion software package[34] to a normal-mode numerical model,[44] the required environmental parameters were extracted from the vocalizations themselves, while simultaneously recovering the best-fit range and depth of the whale. The fitness criteria used were the normalized output of the Bartlett processor, incoherently averaged over 3–10 frequencies between 16 and 130 Hz. Identical global optimization procedures were used for each inversion, which adjusted 18 parameters in an attempt to maximize the peak correlation of the incoherently frequency-averaged ambiguity surfaces. Each inversion was repeated 40 times for each vocalization sample, using a different initial population of trial solutions, and the inversion run that yielded the largest correlation was retained.

Nine of the 18 inverted parameters defined a geoacoustic model of the ocean bottom that assumed a sediment layer overlaying an infinite basement layer. The sediment thickness was set to 70 m, deeper than the expected bottom penetration for all frequencies except possibly 17 Hz. A sediment sound-speed profile was constructed by allowing the inversion to adjust the sediment sound-speed at depths of 23, 46, and 70 m beneath the water/sediment interface, as well as the bottom half-space sound-speed. The sediment sound-speed at the water/sediment interface was allowed to vary between realistic values of 1450 and 4000 m/s, and the sound-speed was allowed to increase between 0 and 1000 m/s every 23 m, ensuring the physically realistic result that the bottom velocity would increase with depth. The inversions did not solve for possible large shear speeds in either the sediment layer or half-space, as the normal-mode models used for the inversion incorporated a perturbation approach to compute shear, which is valid only for small shear values.[2]

Baseline water-borne sound-speed profiles were constructed using temperature data from five XBT casts. The technique of empirical orthogonal functions (EOFs) was applied to enable inversion of the water column sound-speed profile using only a few parameters.[45] The MFP results were insensitive to the exact shape of the sound-speed profile used. The inversion techniques were benchmarked by performing inversions on the Swellex-3[27] data set, where the geoacoustic parameters were already known.

Once acquired, the inversion parameters were used to perform MFP on the rest of the calls in the sequence, while ensuring that updated ''snapshots'' of the vertical array geometry were used. Once a time series was selected, a single global inversion typically took 10–20 min using a Sun Ultra workstation. A MFP computation using the inversion results took 30–60 sec per call, using routines developed in MATLAB.

C. Interpreting inverted array tilt

Imagine a tilted vertical array with a total offset H between the top and bottom hydrophones. Because MFP models the two-dimensional acoustic field between the source and receiver, it is only the projection (H') of the total offset onto the MFP plane that influences the received acoustic field. If the source bearing is the same as the tilt direction, then $H'=H$; if the source bearing is perpendicular to the tilt bearing, then $H'=0$—the projected offset is zero. Because the maximum array tilt and tilt direction were independently measured by an inclinometer, the projected offset can be converted into a rough source bearing estimate. The convention used in this paper is that a negative value of H' indicates the array is tilting away from the source. One important consequence of this behavior is that if the projected array tilt remains constant over time while the range decreases, then the source must be moving toward the array.

II. RESULTS

In this paper all dB units have been expressed in terms of pressure spectral density (*re* 1 μPa^2/Hz), and source levels in terms of source pressure level spectral density (*re* 1 μPa^2/Hz @ 1 m).

A. MFP tracks

1. Case 1—demonstration of an acoustic/visual match

The ocean conditions were calm over the 15-min period shown in Fig. 3, beginning at 14:01 GMT, Julian Day 204, 1996, and are among the last calls recorded during the experiment. The myriad 20–30-Hz pulses that are prominent around 750 sec may be fin whale calls.[46–48] In addition, at least three blue whales are vocalizing during this time, generating two types of signals known to be produced by blue whales.[9,17,18,20,49,50] The broadband pulsed call is conventionally called ''type A,'' and the harmonic FM sweep is labeled ''type B.'' One animal is producing very faint B calls ($\sim$100 dB *re* 1 μPa^2/Hz), with only the 50-Hz tone visible, suggesting that it is greater than 5 km away. Another animal generated the two A-B sequences that begin at roughly 100 and 310 sec along the time axis in Fig. 3. A third animal has produced the intense broadband type A calls recorded at 293, 505, and 718 sec (labeled ''a,'' ''b,'' and ''c'' in the figure), and these calls are the focus of this case. Of the three calls, the 505-sec call has the best signal-to-noise ratio. The 293-sec call is also of good quality, but the 718-sec signal suffers from contamination from pulsing broadband noise and possible fin whale pulses.

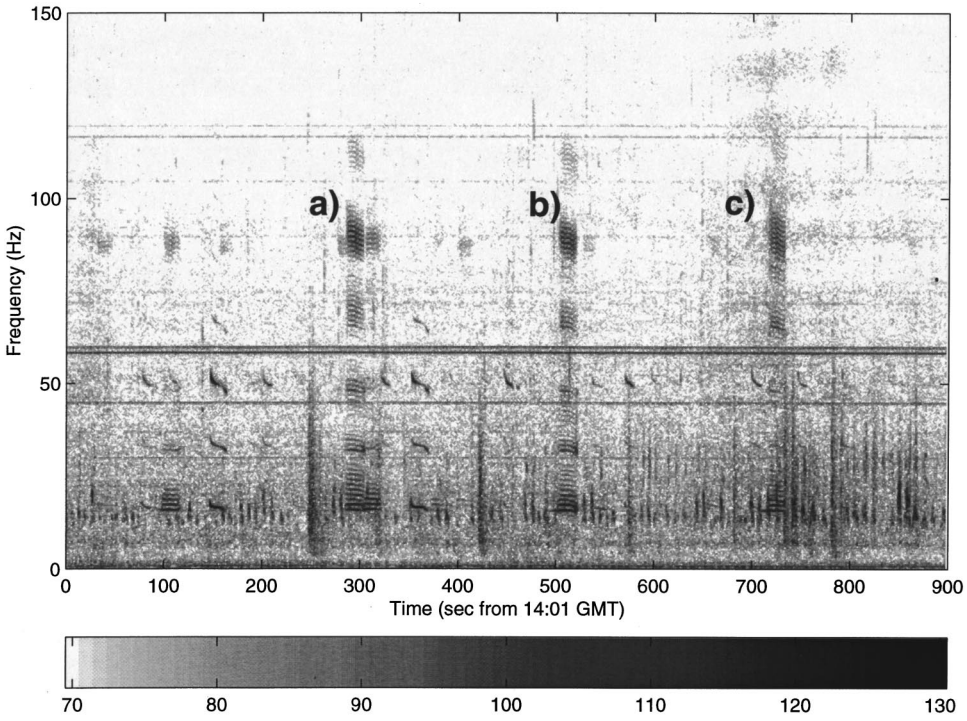

FIG. 3. Spectrogram of case 1, Julian Day 204 time sequence, starting at 14:01 GMT. Power spectral density levels are in units of dB *re* 1 μPa^2/Hz. Note the three strong type A calls at 290 (''a''), 505 (''b''), and 720 (''c'') seconds. The multiple vertical energy bands between 20 and 30 Hz may be fin whale vocalizations.

The inversion procedure was performed on each of the three high-level type A calls, using an incoherent average of 8–10 frequencies between 16 and 112 Hz. The inversion results are graphically displayed in Fig. 4. The inverted sediment sound-speed profiles from the three calls are generally consistent to within ± 50 m/s down to depths of 46 m beneath the surface, with a mean speed around 1621 m/s at the water sediment interface. The accuracy of these geophysical estimates is explored further in Sec. II B.

The multiple arrival paths from a propagating acoustic signal generate an interference pattern in the received pressure field along the array, as a function of depth. To compare the received data from the ''b'' call with that of the best-fit model, the measured vs modeled pressure magnitude across the vertical aperture of the array is plotted in Fig. 5, for six different frequency components. The fit is excellent across a wide range of frequencies, particularly in the high signal-to-noise (SNR) ratio band between 85 and 95 Hz.

The frequency-averaged ambiguity surfaces for each call are displayed in Fig. 6, using the adaptive white-noise constraint (WNC) MFP processor,[51,52] where the constraint has been set to 3 dB below the maximum white-noise gain. The WNC correlation output is generally less than that of the Bartlett processor.

Clues about the whale's azimuthal position are provided by the projected array geometry obtained from the inver-

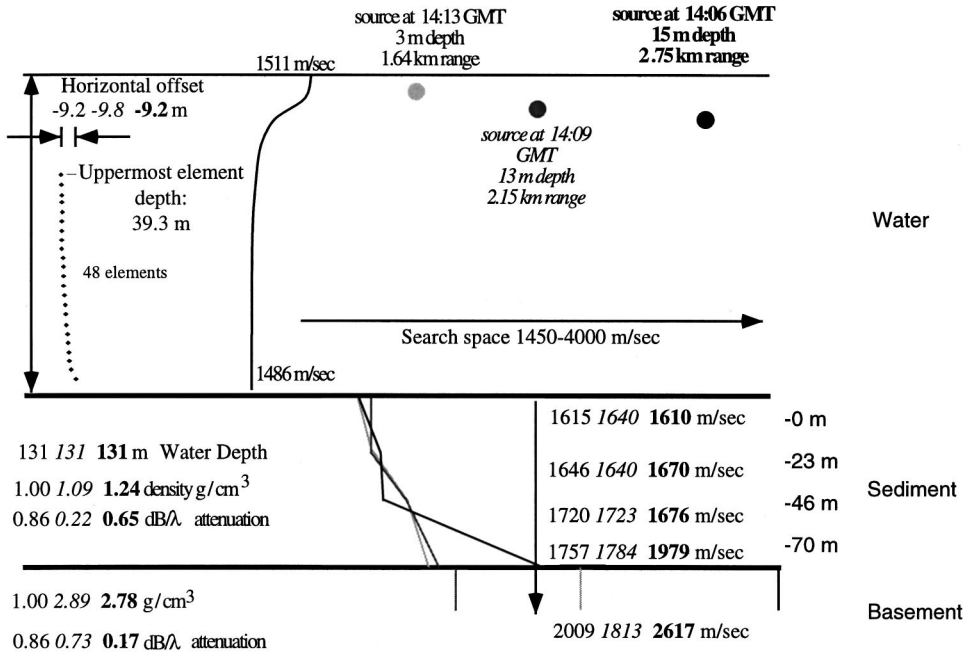

FIG. 4. Illustration of best-fit inversion model for the three type A calls from case 1. Parameters obtained from the same call share the same shading and text style.

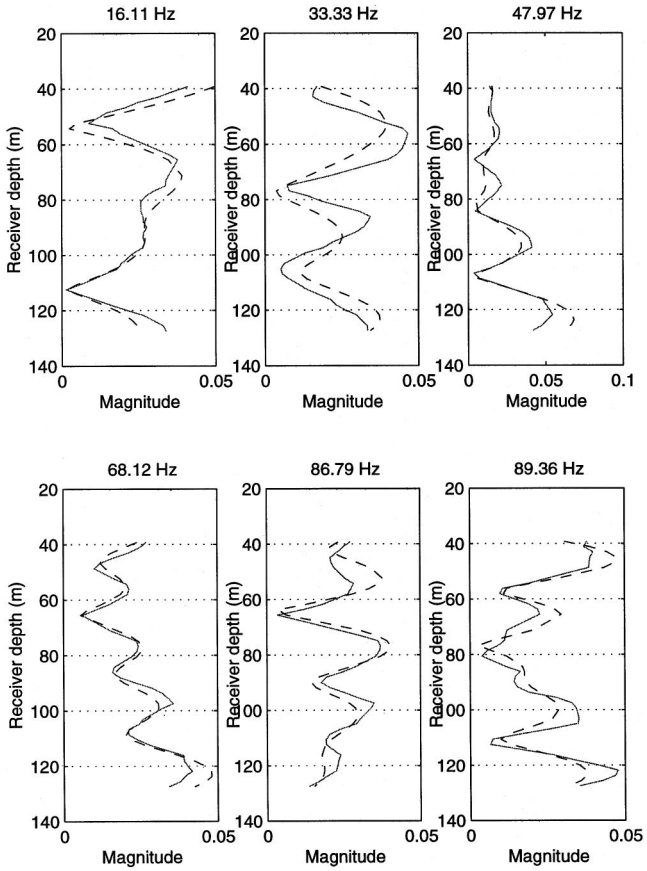

FIG. 5. Comparison between the normalized sound pressure magnitude from the middle type A call (dotted line), and that predicted by the best-fit inversion, as a function of depth for six different frequency components.

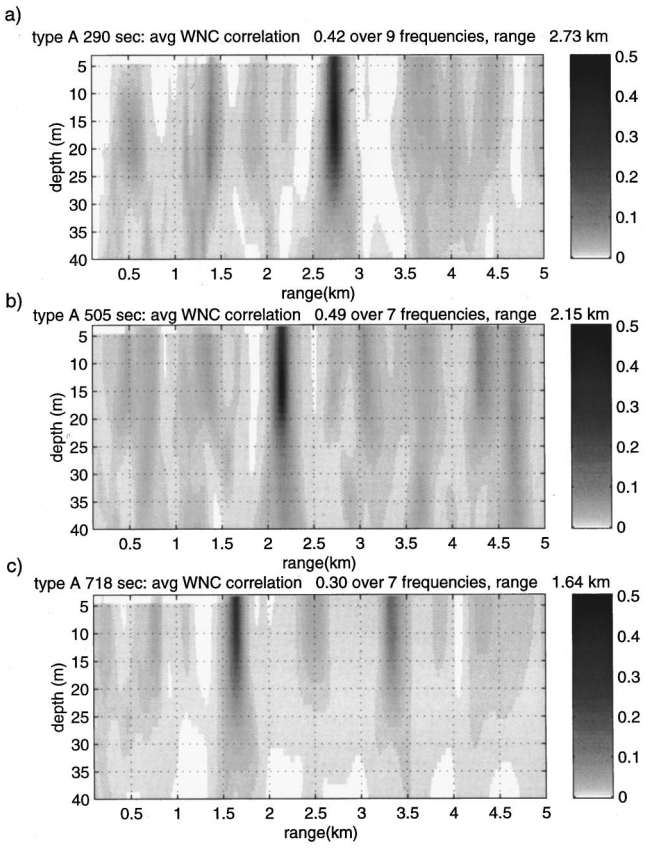

FIG. 6. Ambiguity surfaces from case 1 calls shown in Fig. 3, using the white-noise constraint (WNC) processor. The constraint has been set to 3 dB below the maximum white-noise gain. Frequencies have been selected from the 32-, 48-, 65-, 90-, and 112-Hz bands. Generally correlation values of the WNC are lower than Bartlett values. (a) 290-sec call, average of nine frequencies between 17 and 112 Hz; (b) 505-sec call, average of seven frequencies between 17 and 112 Hz; (c) 720-sec call, average of seven frequencies between 17 and 112 Hz.

sions. For example, the projected horizontal offset H' between the top and bottom hydrophone remained constant at about -9.5 m, so the whale must have been swimming along a radial directly toward FLIP. Had the bearing of the animal relative to FLIP changed significantly during the calling sequence, the inverted array tilt would have changed with time. The negative tilt values indicate the array was tilting away from the whale, and since the array was tilting toward the NW, the bearing of the animal must be to the E or SE. The whale moved 1.1 km over about 430 sec. Its average speed over this time was therefore 2.6 m/s (9.2 km/hr), consistent with estimated swimming speeds between 5 to 33 km/hr for blue whales.[53]

Given the long duration of these calls (around 15 sec), it is possible to perform MFP on sequential time segments within a call, obtaining the animal's dive profile while vocalizing. The ranges and depths from the resulting ambiguity surface mainlobes are plotted in Fig. 7, at 1-sec intervals, for the 505-sec (''b'') call. While calling, the animal's range decreases by 2.5 to 3 m/s, consistent with the long-term swimming speed derived from Fig. 6.

The animal seems to remain at a constant depth over the duration of the 505-sec call, to within the resolution of the MFP processor. This theoretical resolution limit, based on the Cramer–Rao lower bound,[3] is expected to be around ± 2 m in depth and ± 10 m in range, for a 89-Hz signal with a 20-dB signal-to-noise ratio (SNR). Bathymetry mismatch also introduces a depth uncertainty, as the true ocean bottom is not flat. At 2.1-km range, the water depth lies between 110 and 150 m, depending on the azimuth used, which translates into an absolute source depth uncertainty of about ± 3 m[54] and a range uncertainty of about 15%. Thus the relative ranges and depths in Figs. 6 and 7 are probably accurate, but the absolute ranges and depths have uncertainties of ± 3 m in depth and ± 300 m in range.

Both Figs. 6 and 7 suggest a swimming speed of 2.6 m/s toward FLIP. Therefore this whale would have taken about 10.5 min to cover the remaining 1.6 km to the vertical array, suggesting that a visual sighting of an animal from FLIP should have been noted between 14:23 and 14:24 GMT on Julian Day 204. Indeed, this was the case.

Beginning at 14:23 GMT, a videotape of two whales approaching FLIP was recorded using a Cannon Hi 8-mm ES5000 camcorder. During this period, the animals approached from the E/SE, performed a shallow dive (about 30 m away from FLIP), then altered course slightly to swim away to the NW. Scientists at Southwest Fisheries Science Center identified both animals on the videotape as blue whales.[55] If these whales were indeed responsible for the recorded calls, then it seems likely that only one of them vocalized, due to the consistency in style and timing of the

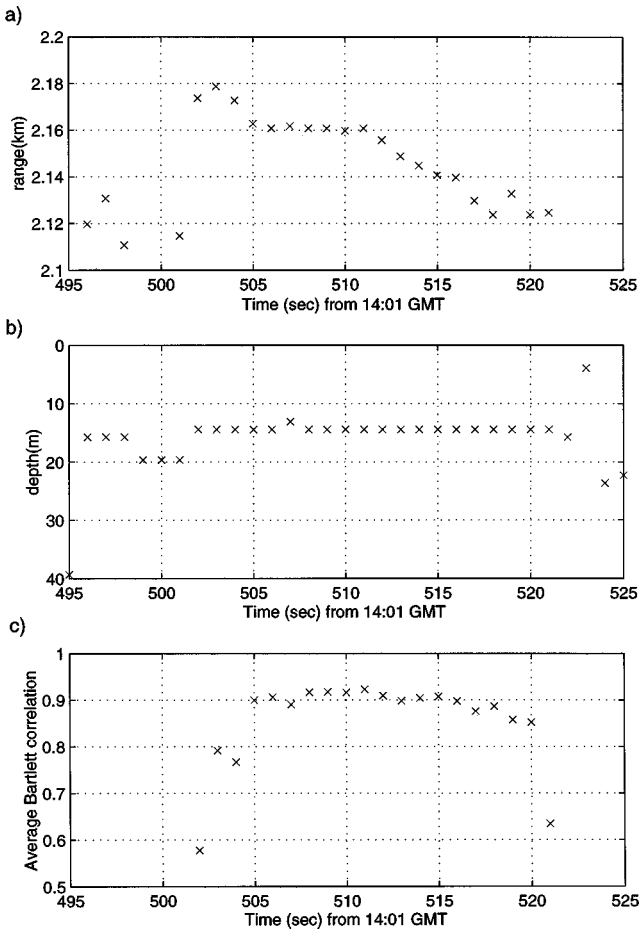

FIG. 7. Estimated changes in (a) range and (b) depth during ''b'' type A vocalization. Seven frequencies between 30 and 120 Hz were used in the MFP processing. Plot (c) shows the average correlation of the MFP peak over time. Estimated Cramer–Rao bound resolution is ± 3 m in absolute depth, ± 10 m in absolute range.

type A calls. One animal was somewhat smaller than the other, so perhaps the pair was a mother and her calf—but this will remain a speculation.

2. Case 2—maximum ranges obtained from MFP

The 90-min sequence analyzed here, beginning at 19:52 GMT on Julian Day 203, demonstrates for the first time how MFP can track calling whales to ranges in excess of 60 water depths, a situation where no direct path between the source and receiver exists. While case 1 analyzed three type A calls over a 15-min period, case 2 contains data from 67 type B and 39 type A calls from two different animals, one out to a range of over 8 km. Azimuthal information provided by a DIFAR sonobuoy was also available during part of the sequence, enabling high-resolution three-dimensional position estimates.

At first, only a single whale called, making type A-B doublet patterns. At approximately 20:36 GMT (44 min into the sequence), a second whale began calling. This animal had a different vocalization pattern, making three to five B calls for every pulsed A call. Both whales called at predictable intervals, and both also had their own characteristic FM downsweeps, making it easy to separate individuals from the spectrograms. For 30 min both animals called simultaneously, before the first whale fell silent at around 21:07 GMT (75 min into the sequence). Fortunately, a DIFAR sonobuoy had begun recording data 5 min earlier, and so precise azimuthal estimates were obtained for both animals. The second animal continued calling for another 15 min before suddenly lapsing into silence shortly past 21:22 GMT. Signal harmonics as high as 135 Hz were detected during this whale's final vocalizations.

Several strong type B calls produced by the second whale around 21:20 GMT (88 min into the sequence) provided excellent inversion sources, due to their high SNR and the presence of many harmonics. The resultant range and depth tracks from both animals, assuming a range-independent bathymetry, are plotted in Fig. 8(a) and (b). Only the 32-, 50-, and 65-Hz frequency bands have been averaged to generate these plots, because they were the only components present in all calls. Incorporating the higher-frequency components, whenever they were present, did not significantly alter these results. Each data point represents a covariance matrix constructed from 4096 pts (2.4 sec) of data. Adjacent data points were spaced 1 sec apart, so a single call yielded 10 to 15 range/depth estimates. Only points whose frequency-averaged peak correlation was greater than 0.7 have been plotted. Because of the higher SNR of the type B tones, the correlations of the type B calls are generally better than the type A estimates.

The first whale was detected at nearly 9-km range, which steadily decreased at a rate of about 8.2 km/hr, again consistent with known swimming speeds. The depth estimates show high scatter until the range became less than 5 km, and then they settle to values between 20 and 30 m. This animal swam within 1.4 km of FLIP at its closet point of approach.

The second whale's behavior provides an interesting contrast, in that its range remained relatively constant over 45 min. Gaps in vocalization are visible, which probably occurred when the animal surfaced. When first detected, the whale's apparent depth was shallow, at around 10 m. Over the next 10 min the source depths increased to a final average value of 20 m, where it remained for the rest of the sequence.

Figure 8(c) shows the best-fit projected array offsets (H') from 17 global inversions, computed at various times from both animals. As discussed in Sec. II C, projected array tilts can be converted to azimuthal estimates if assumptions about the array geometry are made. Because the array was tilting toward the west, the initial negative array offsets indicate that both animals were first detected roughly east of FLIP. The second whale's projected tilt remains fixed between -24 to -26 m, suggesting that its bearing did not change much over this time. By contrast, the azimuth of the first whale changes considerably, as the projected offset shifts from -25 to $+25$ m over 90 min. If the total array offset is assumed to lie between 25 and 30 m, then both whales were first detected at a bearing of around 95°, almost due east of FLIP. The first (transiting) whale reached its closest approach to FLIP at roughly 330° bearing, and stopped calling at approximately 315° bearing. The second whale, whose apparent bearing never changed, had a final estimated bearing of $105 \pm 40°$. The DIFAR results from this

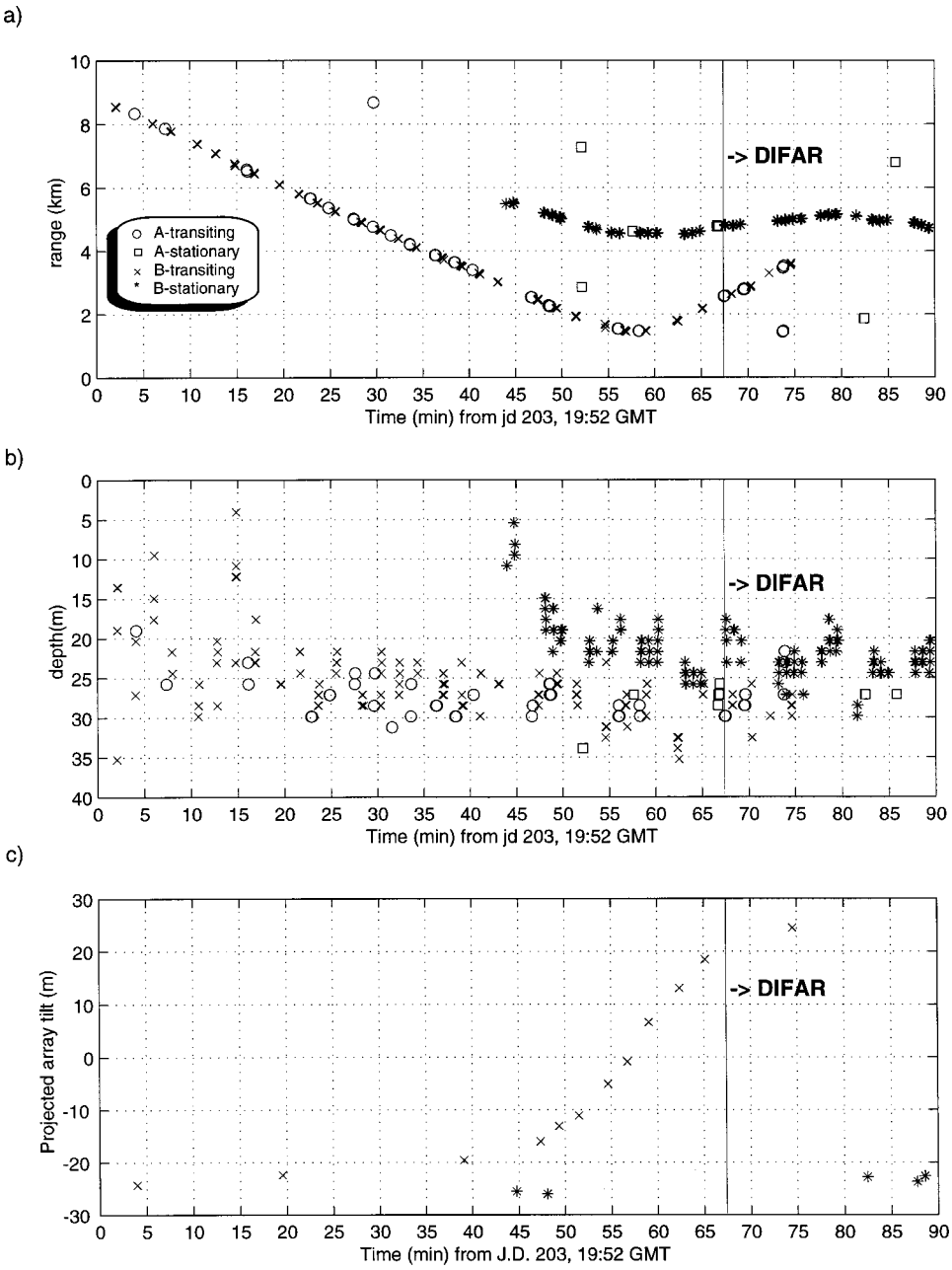

FIG. 8. Computed ranges and depths from case 2, for two animals over 90 min, starting from 19:52 GMT on J.D. 203. The 32-, 50-, and 65-Hz frequency bands were used in the MPF processing, assuming a range-independent bathymetry. A DIFAR sonobuoy begins recording data at 21:01 GMT. Each data point represents 2.5 sec of data, spaced 1 sec apart within a call. (a) range versus time; (b) depth versus time; (c) inverted horizontal array offset versus time. Whale bearing can be estimated from array offset.

time confirmed the second whale was calling from a bearing of 105°, and that the final bearing of the transiting whale was 340°. Both measurements thus agree with the rough inverted-array tilt predictions.

Because the azimuths of these calls were available, the effects of incorporating a more accurate bathymetric profile could be evaluated. For example, the true bathymetry along a 105° bearing from FLIP changes from 133 to 118 m over 5 km. When range-dependent replicas were recomputed using a parabolic-equation model,[56] the second whale's range estimate became 4.6 km, instead of the 5-km range obtained from assuming a flat bottom. The estimated depth also became about 2 m shallower, in agreement with theoretical expectations.[54] The effects of range-dependent bathymetry were therefore concluded to be mild for animals approaching from the east, or for animals less than 3 km away from FLIP.

3. Case 3—close approach with unusual vocal behavior

Case 3, the hour-long sequence analyzed here, began with a single type A-B doublet recorded on Julian Day 204, 1996, at 8:30 GMT. After a 10-min gap, two strong bouts of unusual calls appeared, lasting about 14 min. These vocalization bouts were striking in their variety. Each FM sweep had a different modulation, from straightforward downsweeps to U-shaped contours. The animal switched between type A-B doublets and type A calls followed by multiple Bs.

Between 29 and 30 min, the whale generated several heavily modulated type B calls and two unusual FM (''type D^{10}'') sweeps, which are plotted in Fig. 9(a). The whale made a third type D call around 100 sec later, then continued calling before lapsing into another 6-min period of silence beginning around 34 min. At 40 min, the animal generated

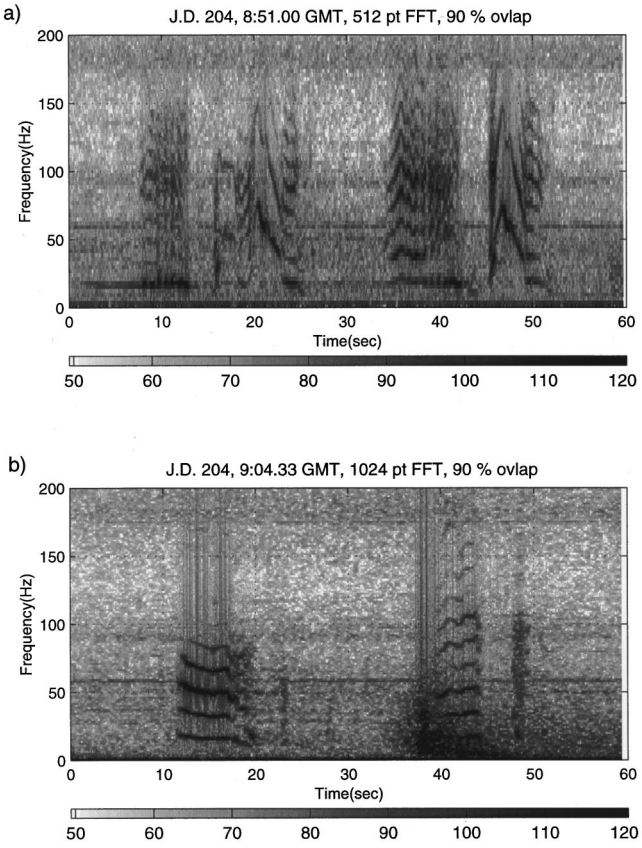

FIG. 9. Spectrograms of 60-sec segments of unusual calls recorded during case 3, expressed in units of pressure spectral density (dB *re* 1 μPa^2/Hz @ 1 m). Both sets of calls were produced when the animal was near the bottom of its dive profile: (a) Strongly modulated type B and D downsweeps, beginning at 8:51 GMT; (b) other examples of highly modulated calls, beginning at 9:04:30 GMT.

two more bouts of vocalizations, separated by an apparent breathing gap at 45.5 min. Some examples of calls generated over a 1-min period during the last bout are shown in Fig. 9(b). The whale finally fell silent at 55 min, or 9:17 GMT.

Figure 10 shows the final MFP results for this track, assuming a flat bathymetry. As with Fig. 8, the results displayed here use frequency components picked from the 32-, 50-, and 60-Hz bands, each point represents an analysis of 2.4 sec of data, and adjacent points are spaced 1 sec apart. By using only these three frequency components, all calls could be included. Using higher-frequency components, when available, did not change the localization estimates.

Figure 10(a) shows the isolated type A-B doublet was generated at around 3 km range, at around 30-m depth. The first strong vocalization bout started at 1.67-km range, which steadily decreased at an average rate of 1.5 m/s to a minimum range of 386 m, after which the whale ceased calling. After the 6 min gap, the animal produced two more calling bouts, both showing the animal's range now increasing. The animal's radial velocity seemed to increase from 0.58 to 1.23 m/s between the two bouts. The last fix on the animal yielded a range of 1.24 km, after which it fell silent.

The depth estimates in Fig. 10(b) show four complete dive profiles. The scatter of adjacent data points (± 4 m) is consistent with theoretical predictions at these frequencies and ranges. Generally, the animal began calling at 20-m depth, and over 2–3 min descended to a depth of 30 to 35 m. After holding this depth for another 2–3 min, the animal began ascending while continuing to vocalize. The final calls were made between 15- to 20-m depth, with an estimated depth resolution of ± 5 m. The animal took about 2 min to surface and breathe, before descending for the next calling bout.

Figure 10(c) shows the inverted projected array offsets of the vertical array. The projected array tilt remained constant at -10 m as the animal approached FLIP, except for a small excursion at 20 min. At this time the array was leaning WNW, so the animal must have arrived from an easterly bearing, similar to those obtained in the previous sections. The constant projected tilt indicated the animal was swimming directly toward FLIP, just like the two whales in case 1. After the 6-min calling gap, the third calling bout produced a projected array tilt of 0, indicating that the animal had veered off to the side of FLIP, increasing its range to 490 m. The increasing positive tilt values following this time suggest that the animal had swum past FLIP, steadily changing its bearing with respect to FLIP, and thus swimming along a different route than its earlier approach.

Separate estimates of the whale's bearing were obtained by converting the projected array tilt into a bearing estimate (Sec. I C), and by using range-dependent MFP runs to obtain the best-fit bathymetry profile between FLIP and the whale, which can be converted into a bearing estimate.[57] The combined analyses suggest the whale arrived from a bearing between 80 and 120°, while swimming directly toward FLIP to within a range of 390 m. The animal then veered to the north, and may have swum a partial circle around FLIP, before finally swimming toward 340–350°. Thus the initial and final bearings of this whale are similar to those obtained from the transiting whale in case 2. However, this whale clearly made a course correction to avoid FLIP.

B. Evaluation of geoacoustic inversion results

This section summarizes the results from the 48 geophysical inversions extracted from the whale vocalizations discussed in cases 1–3, and compares the estimated sediment speeds with those expected from core samples collected from the region. Most inversions used type B calls, due to their high SNR ratio. Each inversion also optimized the waterborne sound-speed profile, but the results were relatively insensitive to the details of the profile shape. The low frequencies used in the inversion were probably the reason for this insensitivity; for frequencies greater than 150 Hz, the sound-speed profile structure should have more influence on the vertical field structure.

The most important geoacoustic inversion parameters were the sediment sound-speeds at the water/sediment interface, and at depths of 23, 46, and 70 m beneath this interface. The inversion also solved for the best-fit sediment density and attenuation, and for the speed, density, and attenuation of the acoustic half-space that was assumed to lie beneath the sediment. The half-space properties will be ignored here, because the acoustic field energy was not expected to penetrate deeper than 70 m. The inversion results confirmed this ex-

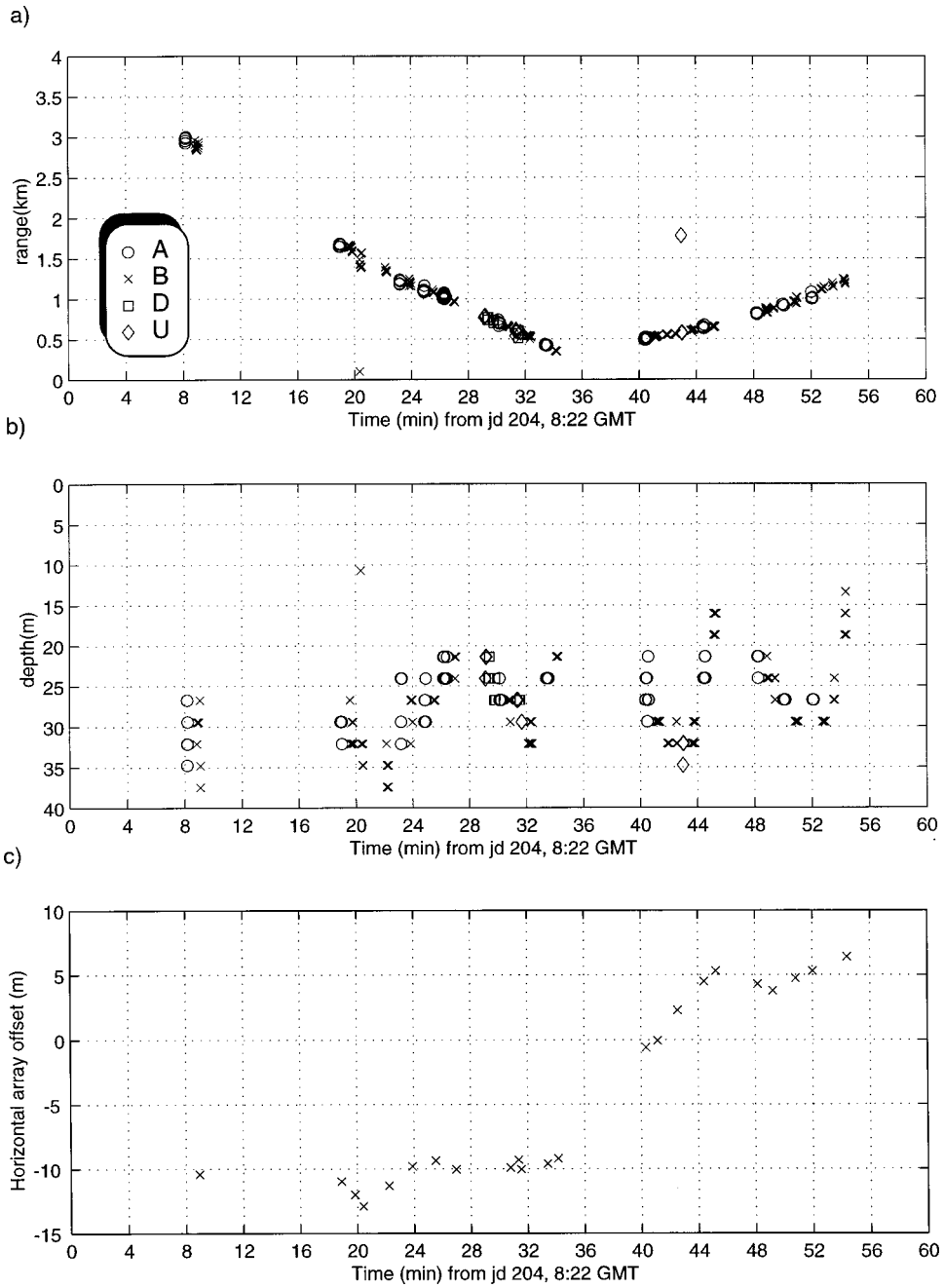

FIG. 10. MFP track of case 3. The track was generated using the 34-, 50-, and 67-Hz signal components, assuming a range-independent bathymetry. Each data point represents 2.5 sec of data, spaced 1 sec apart. The ''U'' label represents highly modulated type B calls. (a) Blue whale range; (b) blue whale depth; (c) projected horizontal array offset estimated from global inversions.

pectation: the inverted half-space parameters were essentially randomly distributed.

The inversions assumed sediment properties were not a function of source location. In reality the bottom was heterogeneous, so the results presented here represented a range-averaged estimate of the bottom properties between each source and FLIP.

Figure 11 displays the inverted interface sediment sound-speeds as both a function of range from FLIP and the whale used as the inversion source. As discussed previously, the precise azimuths of the calling whales were difficult to determine, except when DIFAR sonobuoy data were available. However, each inversion indicated whether a particular call arrived from the east or west, by combining the projected array tilt with knowledge of the array tilt direction. Figure 11 incorporates this information by plotting easterly data as negative ranges, and westerly data as positive ranges.

This sound-speed parameter was allowed to vary between 1450 m/s (representative of water-saturated mud) and 4000 m/s (typical basalt values) during the inversions. Despite this wide range, all inversion results lie between 1550 and 1800 m/s, with 75% lying between 1600 and 1700 m/s, or 4% of the allowed search space. These values are associated with silty/sandy bottoms.[58] Inversions obtained from the same animal over a small range interval also yielded consistent results; the scatter of these adjacent inversion points is about ± 25 m/s. The scatter is much larger between different cases at similar ranges, because the animals are probably calling from different bearings, and the acoustic energy is sampling different sediment profiles. There was no obvious correlation between the spread of the results and the number of frequencies used in the inversion. One might have ex-

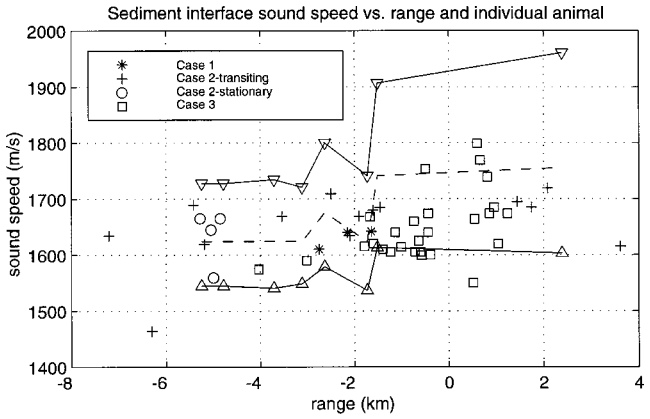

FIG. 11. Inversion results for sediment interface speed, as a function of inversion range and whales used as the acoustic source. The dashed line shows the sound-speeds derived from sediment core mean grain sizes. The solid lines show the sound-speeds computed from grain sizes one standard deviation from the mean. Triangles indicate the ranges of the core samples from FLIP. Negative ranges represent locations east of FLIP, and positive ranges are to the west. The ''stationary'' whale mentioned in the legend refers to the animal in case 2 that held its bearing fixed at a steady range of about 5 km.

pected the precision to increase as higher-frequency components are included; however, higher frequencies also penetrate less deeply into the sediment, and thus involve a different spatial average.

The recovered surface sediment speed is the only geoacoustic parameter for which independent information exists, in the form of sediment cores collected in the region by various institutions, particularly the United States Geological Survey (USGS) and the University of Southern California (USC)[59] over the past several decades. The penetration depth of these cores is generally less than a meter.

The sediment core data report the grain size distribution using a logarithmic measure $\varphi = \log_2$ (grain size in mm). Considerable variation exists in the particle sizes within a particular sample, so both the mean and standard deviation of φ are recorded. Sediment grain sizes can be converted to bottom sound-speed estimates via an empirical fit,[60] using a measured water sound-speed of 1485 m/s. Three sediment sample speeds are plotted in Fig. 11. The dashed line uses the mean φ, and the two solid lines use φ values lying one standard deviation on either side of the mean. The triangles indicate the ranges of the individual cores from the FLIP position. The plotted core data are restricted to those obtained within 8 km of FLIP, in water depths between 100 and 200 m. The reason for restricting the water depth is that there is a correlation between water depth and sediment sound-speed. For example, as the water shallows while approaching San Miguel shore, both the particle size and sediment sound-speed increase. Even with this depth restriction, the sediment sound-speed apparently changes west of FLIP. Part of this change may reflect the fact that only one core is available west of FLIP (for some reason a gap in sampling occurs to the west in an otherwise well-covered area).

East of FLIP, the whale inversion data lie within ± 50 m/s of the average sediment core sound-speed. The inversions underestimate the mean sound-speed between -1 and $+4$ km range, but this comparison is based on only two sediment cores. In general, the inversion results show a good match with the limited ground truth information available, particularly considering that the animals' bearings are imperfectly known.

Table I summarizes the properties and locations of the sediment cores used in this section. The ''AHF#'' column refers to the indexing system used by USC to record their samples.

C. Source level estimates

Using the range and depth information in Figs. 8 and 10, multichannel deconvolution techniques[15,16,61] were applied to estimate the source levels of the harmonic frequencies for the three whales in cases 2 and 3. Because the whales' acoustic power output varied considerably during a single vocalization, it is necessary to perform multiple estimates per call to estimate the maximum source levels.

Figure 12 displays the source spectral density levels (dB *re* 1 μPa^2/Hz @ 1 m) for the five lowest-frequency harmonics of the whales in case 2. To convert spectral densities into tonal spectral level, 4 dB should be subtracted from these values (to account for the 0.4-Hz frequency bin width). The uncertainty in these estimates are about ± 5 dB.

Some interesting results are that the 50-Hz tone source level is within 5 dB of the 17-Hz tone level, and that both animals consistently maintain a maximum source spectral density level of about 185 dB *re* 1 μPa^2/Hz @ 1 m (thus total power between 10–100 Hz is about 180 dB *re* 1 μPa @ 1

TABLE I. Sediment core interface sound-speed estimates, based on a water sound-speed of 1485 m/s.

AHF#	Latitude	Longitude	Range (km) from FLIP	Water depth (m)	φ	Skewness	Expected sound-speed (m/sec) over ± 1 standard deviation: Min.	Mean	Max.
24237	33.97	120.45	1.51	169	2.3 ± 2.1	1.3	1613	1741	1907
24238	33.967	120.433	2.63	135	3.3 ± 1.8	2	1579	1676	1741
24239	33.968	120.418	3.71	128	4.2 ± 1.8		1540	1624	1735
23159	33.983	120.435	1.73	115	4.2 ± 1.9	2	1537	1624	1742
23163	33.983	120.42	3.11	107	4.2 ± 1.6	6.5	1548	1624	1721
23164	33.985	120.402	4.78	100	4.2 ± 1.6		1548	1624	1727
23184	33.968	120.400	5.24	115	4.2 ± 1.7	2.5	1544	1624	1728
25192	34.00	120.47	2.39	110	2.1 ± 2.5	0.5	1608	1761	1968
FLIP	33.98	120.454		130					

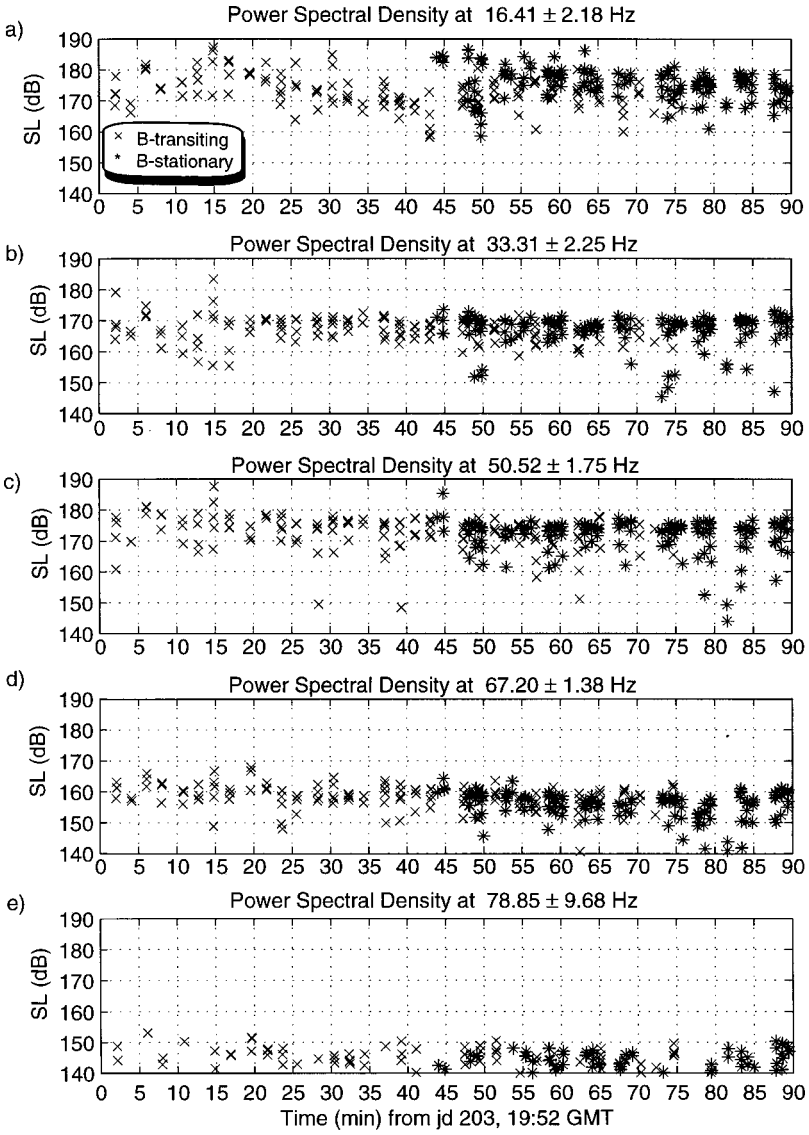

FIG. 12. Blue whale type B call source levels for case 2, estimated using locations given in Fig. 8. Levels are given in terms of pressure spectral density (dB *re* 1 μPa^2/Hz @ 1 m). (a) 16-Hz band; (b) 32-Hz band; (c) 51-Hz band; (d) 67-Hz band; (e) 79-Hz band.

m). In addition, 43 min into the sequence both animals were calling within 2 km of each other, yet neither animal appeared to alter its movements or vocalization patterns in response to the other's presence.

The source levels estimated from case 3 are plotted in Fig. 13. The 17-Hz tones are surprisingly weak, reaching a typical spectral density level of only 160–170 dB *re* μPa^2/Hz @ 1 m, around 10 dB weaker than the levels plotted in Fig. 12. However, the source levels of the harmonics are similar for both cases.

D. Source signature recovery for case 3

Precise knowledge of a blue whale's acoustic location allows not only the source levels to be recovered, but also the relative phase between frequency components of a call. Thus the original time series produced by the whale can be estimated, using multichannel deconvolution methods.[15,16,61]

During its final dive before passing FLIP, this whale generated three strong ''type D'' FM downsweeps,[10] plotted in Fig. 9(a). Single-element spectrograms of these signals revealed interesting narrow-band regions of high intensity levels between 60 and 120 Hz. To verify that these regions were not products of waveguide propagation effects, as might be reasonably expected,[62] the source time signatures were estimated for the three calls using a Gauss–Markov estimate [Eq. (4) in Ref. 15]. Calibrated spectrograms of these reconstructed signal estimates are shown in Fig. 14, where the gray scale is in units of source pressure spectral density (dB *re* μPa^2/Hz @ 1 m). The theoretical depth resolution of the MFP results presented here is expected to be within ± 2 m, because frequencies greater than 110 Hz were used in the inversions.

These narrow-band high-intensity regions (indicated by white arrows) are not propagation effects, but seem to be generated within the animal itself. Whenever a harmonic of the FM fundamental passes through this region, the signal level increases by around 5–10 dB.

III. DISCUSSION AND SPECULATIONS

A. General comments

The four whales tracked in this paper provide interesting insights into their acoustic behavior. While blue whales are capable of descending to 100-m depth to feed,[38] all the

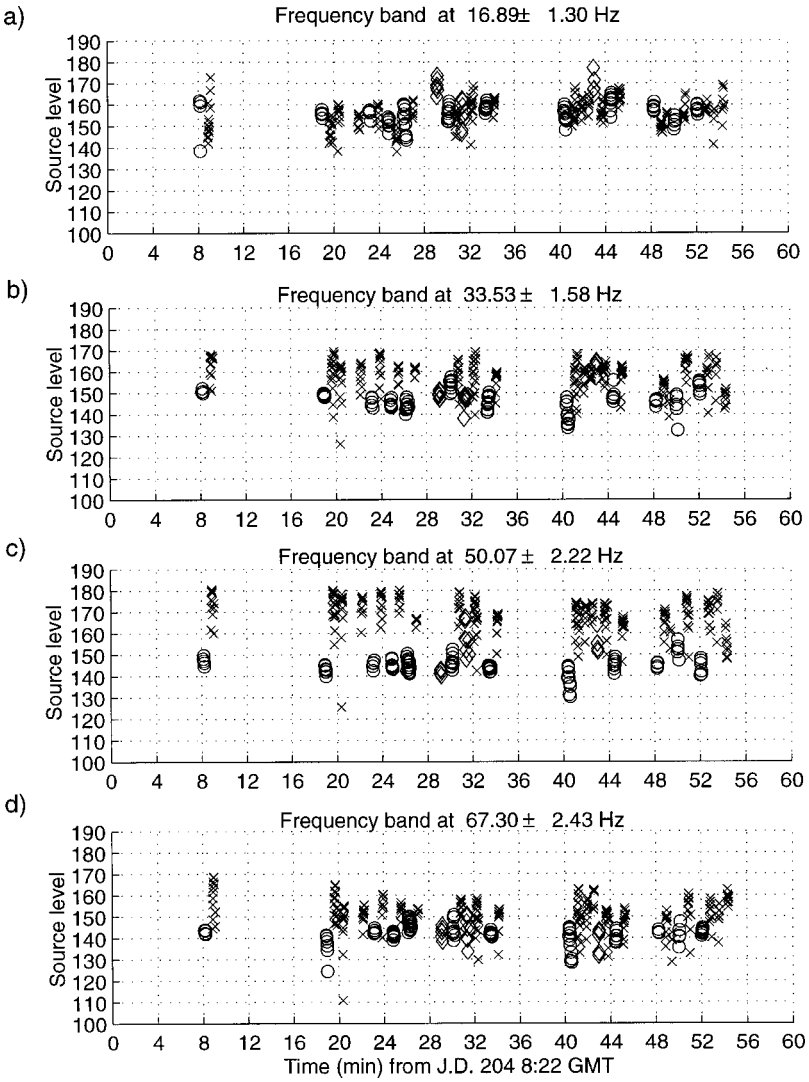

FIG. 13. Estimated source pressure spectral densities in different frequency bands of type A and B calls (dB *re* 1 μPa^2/Hz @ 1 m) for case 3. Call locations were estimated using 30-, 50-, and 65-Hz band information. Circles represent type A calls, ''×'' represents type B, and diamonds represent strongly modulated B and D calls. (a) 17-Hz band; (b) 33-Hz band; (c) 50-Hz band; (d) 67-Hz band.

whales tracked here vocalized between 10- and 40-m depth, whether stationary or transiting. The animal in case 3 yielded four complete dive profiles that show the animal's depth changes only gradually while calling. Most animals swam from east to west at rates of around 2–3 m/s, but one animal remained within 500 m of its original position for 45 min. The case 2 sequence tracked two vocalizing whales simultaneously, including a period when the animals passed within 2 km of each other. However, neither animal appeared to alter its course in response to the other's presence.

Having constructed an environmental propagation model, it is a simple matter to compute both the optimal frequency of propagation, and the depth at which an acoustic source should be placed to minimize transmission losses.[63] The optimum depth for transmitting frequencies between 10–150 Hz in a 130-m deep environment is about 80 m. Over a 10-km propagation range, a 17-Hz source shallower than 40 m would suffer a large transmission loss due to destructive interference between the source and surface reflection. Given the fact that most of the energy in blue whale vocalizations lie under 20 Hz, it seems clear that the vocalization depths of the animals were not acoustically optimized for propagation under the shallow-water conditions present around FLIP.

B. Do blue whales display an internal resonance?

The results of Sec. II D suggest the presence of a possible internal resonance within the animal. A mechanical resonance might be present in the oscillating source (generally assumed to be or near the arytenoid cartilages, see references in Ref. 64), or an air-filled space may act as a resonator that couples with the oscillator, similar in manner to the way the vibration of the double reed within an oboe is influenced by the resonant characteristics of the tube.[65]

The limited samples present here suggest an air-filled resonator may be more likely, because the frequency of this hypothetical resonance seems to increase with the animal's depth, which is what would be expected if an air-filled cavity were being compressed. Unfortunately, the depth-frequency relationship visible does not fit any simple resonator model. For example, the resonant frequency of a bubble of fixed size is proportional to the square root of the external pressure.[66] The first and last call depths are 20 and 30 m, so the resulting external water pressure increase is about 33%, and the expected frequency shift for a resonating bubble is 15%. The regions indicated by the arrows show a much greater frequency shift. In fact, the hypothetical resonance frequency seems to be proportional to the external pressure squared,

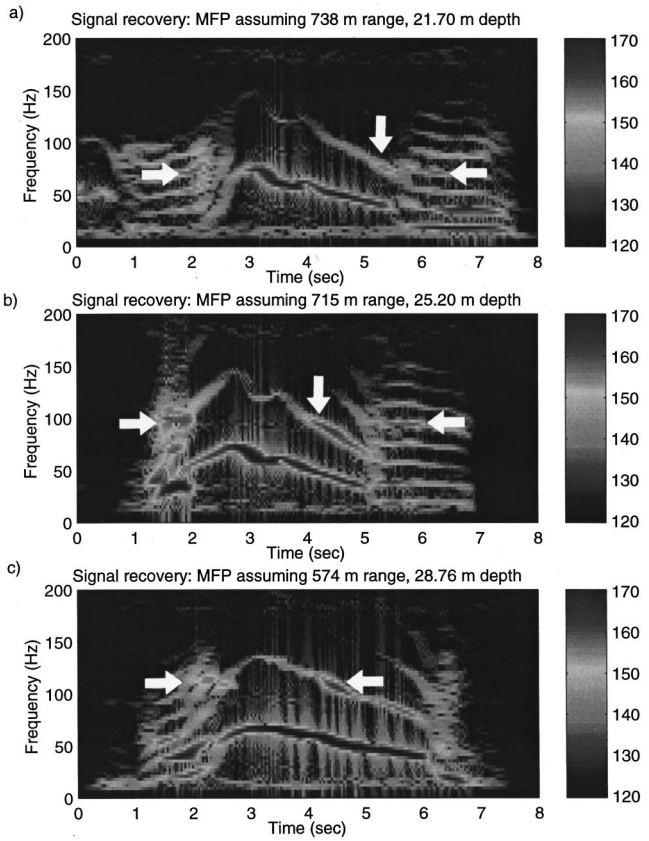

FIG. 14. Source pressure spectral density spectrograms (*re* dB *re* 1 μPa^2/Hz @ 1 m) of estimated source signatures for three ''type D'' FM downsweeps, obtained using multichannel deconvolution and an optimized inverted environment. White arrows indicate speculated resonances of sound-production mechanism: (a) Starting at J.D. 204, 8:51:18 GMT, 738±10 m range, 22 ±2 m depth. (b) Starting at J.D. 204, 8:51:45 GMT, 715±10 m range, 25 ±2 m depth. (c) Starting at J.D. 204, 8:53:28 GMT, 574±10 m range, 29 ±2 m depth.

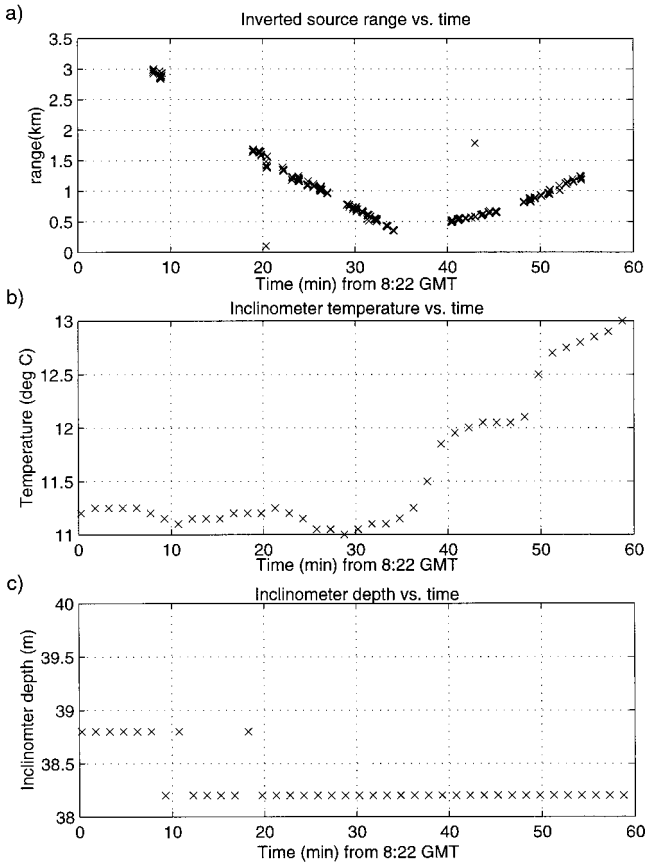

FIG. 15. Comparison between case 3 whale location and local environmental conditions. (a) Range track of blue whale versus time; (b) water temperature (°C) measured at inclinometer versus time; (c) measured inclinometer depth versus time.

instead of the square root. A Helmholtz resonator[66] would also show the same square root dependence on ambient pressure, and a bubble resonator allowed to collapse in volume with depth would still only show a linear dependence on external pressure. It is clear that more samples of these FM downsweeps would be required to answer these questions.

C. Do whales associate with tidal bores?

Another interesting feature associated with case 3 is that the animal's arrival corresponds with a sudden change in oceanic conditions. Figure 15 demonstrates this association by replotting the whale's range versus time in (a), the water temperature at the array inclinometer vs time in (b), and the inclinometer depth in (c). This last plot shows that the temperature change is not caused by a sudden change in the temperature sensor depth (note that the inclinometer depth measurements are quantized in increments of about 0.5 m).

To within the timing resolution of the inclinometer (90 s), the point at which the whale reached its closest approach to FLIP was associated with a 1.0 °C jump in water temperature, followed 10 min later by another 1.0 °C jump. The eventual total temperature increase is 2.5 °C over 30 min. During the previous 11 hours the temperature had remained within 0.5 of 11 °C. This temperature jump was the largest short-term temperature change recorded over the 42 hours of the experiment, and was accompanied by a rapid rotation in the array tilt direction from 300° bearing to about 200°. Unfortunately, heavy cloud cover in the area blocked any useful SST satellite measurements recorded at this time.

An examination of the complete temperature/array tilt record showed that three strong disturbances occur approximately every 12 hours, during which the water temperature rises quickly, and the array tilts to the south. The closest approach of the transiting whale in case 2 also took place in the middle of the previous strong disturbance. These disturbances last less than 2 hours, and then the ocean returns to baseline conditions. The 12-hour spacing of these events suggests a tidal mechanism, during times when the tide level is changing most rapidly. Such behavior might be associated with tidal bores generated along the shelf of San Miguel.[66]

There is anecdotal evidence[67] relating the sightings of whales and other sea life with the presence of strong ocean fronts. Recent work has shown that shorward-propagating internal bores concentrate zooplankton,[68] a propperty that might be exploited by a whale. However, more observations will be required to establish whether whales feed along tidal bores.

IV. CONCLUSION

Matched-field processing (MFP) and global inversion methods have been used to plot the three-dimensional trajec-

tories of four blue whales over periods of up to 90 min and ranges to 8 km. The information needed for the computational models was extracted from the whale calls themselves, using as few as eight hydrophones, spread over a 90-m depth. The extracted values for surface sediment sound-speed estimates lie within ± 50 m/s of those derived from sediment samples collected in the area. These results are believed to be the first successful three-dimensional localizations of a vocalizing baleen whale over long periods of time, and the first successful three-dimensional localizations of marine mammal vocalizations recorded at ranges greater than several water depths from the hydrophone.

The MFP localization and source signature recoveries have raised several interesting questions about the purpose and production mechanism for these calls. The whale in case 3 produced heavily modulated signals that were not stereotyped, atypical behavior for blue whales in this region. In addition, the source level of its fundamental frequency was nearly 20 dB lower than the whales in case 2. These two feature suggest the possibility that this animal might have been a juvenile. This whale's arrival also closely coincided with the arrival of a prominent but short-lived ocean disturbance that changed the ocean temperature by over 2.0 °C over 20 min. Finally, certain FM downsweeps made by this animal display signs of an internal resonance that may be depth-dependent.

Clearly much remains to be learned about the natural acoustic lives of baleen whales, as well as their responses to short- and long-term anthropogenic activities. We hope the potential of some powerful new tools to address these questions has been demonstrated.

ACKNOWLEDGMENTS

The authors would like to thank MPL technical staff and the crew of the R/P FLIP for making the collection of the data used in this paper possible. In particular, the assistance of James Murray and Dave Ensberg is particularly appreciated. They would also like to thank myriad individuals within the Southwest Fisheries Science Center, including Paul Fielder, Alexandra von Saunder, Wayne Perryman, and Jay Barlow. Stu Smith of the Geological Data Center at Scripps provided us with bathymetric information, and useful sediment data was provided by Donn Gorsline of the Department of Marine Geology of the University of Southern California. Peter Gerstoft wrote the extremely useful genetic algorithm inversion package SAGA, and provided a great deal of advice on how to use it. Lisa Schlender of Cascadia Research tried to identify the individual whales videotaped on Julian Day 203. Mike Porter, Mark McDonald, and Dave Mellinger contributed helpful suggestions and insights to the paper. Demultiplexing of the DIFAR sonobuoy data was conducted using software acquired from Greeneridge Sciences, Inc., in Santa Barbara, California. This research was funded by the Office of Naval Research Grant Nos. N00014-97-0593 and N00014-96-1-0603.

[1] A. B. Baggeroer, W. A. Kuperman, and P. N. Mikhalevsky, ''An overview of matched field methods in ocean acoustics,'' IEEE J. Ocean Eng. **18**, 401–424 (1993).

[2] F. B. Jensen, W. A. Kuperman, M. B. Porter, and H. Schmidt, *Computational Ocean Acoustics* (AIP, New York, 1994).

[3] A. B. Baggeroer, W. A. Kuperman, and H. Schmidt, ''Matched field processing: Source localization in correlated noise as an optimum parameter estimation problem,'' J. Acoust. Soc. Am. **83**, 571–587 (1988).

[4] G. D'Spain, W. A. Kuperman, W. S. Hodgkiss, and L. P. Berger, ''3-D localization of a blue whale,'' Scripps Institution of Oceanography, Technical Memorandum MPL TM 447 (1995).

[5] G. L. D'Spain, W. A. Kuperman, W. S. Hodgkiss, and L. P. Berger, ''Three-dimensional localization of a blue whale using broadband matched-field processing for range and depth, and plane-wave adaptive beamforming for azimuth,'' J. Acoust. Soc. Am. **97**, 3353 (A) (1995).

[6] G. L. D'Spain, W. A. Kuperman, C. W. Clark, and D. K. Mellinger, ''Simultaneous source ranging and bottom geoacoustic inversion using shallow water, broadband dispersion of fin whale calls,'' J. Acoust. Soc. Am. **97**, 3353 (A) (1995).

[7] ''Sonobuoy Instruction Manual,'' Naval Weapons Support Center NAVAIR 28-SSQ-500-1 (1983).

[8] K. M. Stafford, C. G. Fox, and D. S. Clark, ''Long-range acoustic detection and localization of blue whale calls in the northeast Pacific Ocean,'' J. Acoust. Soc. Am. **104**, 3616–3625 (1998).

[9] M. A. McDonald, J. A. Hildebrand, and S. C. Webb, ''Blue and fin whales observed on a seafloor array in the Northeast Pacific,'' J. Acoust. Soc. Am. **98**, 712–21 (1995).

[10] A. M. Teranishi, J. A. Hildebrand, M. A. McDonald, S. E. Moore, and K. M. Stafford, ''Acoustic and visual studies of blue whales near the California Channel Islands,'' J. Acoust. Soc. Am. **102**, 3121 (1997).

[11] M. A. McDonald and C. G. Fox, ''Passive acoustic methods applied to fin whale population density estimation,'' J. Acoust. Soc. Am. **1015**, 2643–2651 (1999).

[12] W. A. Watkins and W. E. Schevill, ''Sound source location by arrival times on a non-rigid three-dimensional hydrophone array,'' Deep-Sea Res. **19**, 691–706 (1972).

[13] L. E. Freitag and P. L. Tyack, ''Passive acoustic localization of the Atlantic bottlenose dolphin using whistles and echolocation clicks,'' J. Acoust. Soc. Am. **93**, 2197–2205 (1993).

[14] D. E. McGehee, ''1997 Sperm Whale Abundance and Population Structure Cruise Leg II Sonobuoy Project, Final Report,'' Tracor Applied Sciences T-97-56-0002-U (1997).

[15] S. Finette, P. C. Mignerey, and J. F. Smith, ''Broadband source signature extraction using a vertical array,'' J. Acoust. Soc. Am. **94**, 309–318 (1993).

[16] P. C. Mignerey and S. Finette, ''Multichannel deconvolution of an acoustic transient in an oceanic waveguide,'' J. Acoust. Soc. Am. **92**, 351–364 (1992).

[17] J. A. Rivers, ''Blue whale, *Balaenoptera musculus*, vocalizations from the waters off central California,'' Marine Mammal Science **13**, 186–195 (1997).

[18] P. O. Thompson, L. T. Findley, O. Vidal, and W. C. Cummings, ''Underwater sounds of blue whales, *Balaenoptera musculus*, in the Gulf of California, Mexico,'' Marine Mammal Science **12**, 228–293 (1996).

[19] A. Alling, E. M. Dorsey, and J. C. D. Gordon, ''Blue whales (*Balaenoptera musculus*) off the Northeast Coast of Sri Lanka: Distribution, feeding and individual identification,'' in *Cetaceans and Cetacean Research in the Indian Ocean Sanctuary*, United Nations Mar. Mammal. Tech. Rep. 3, edited by S. Leatherwood and G. P. Donovan (Nairobi, Kenya, 1991), pp. 248–258.

[20] W. C. Cummings and P. O. Thompson, ''Underwater sounds from the blue whale, *Balaenoptera musculus*,'' J. Acoust. Soc. Am. **50**, 1193–1198 (1971).

[21] P. L. Edds, ''Vocalizations of the blue whale, *Balaenoptera musculus*, in the St. Lawrence River,'' J. Mammal. **63**, 345–347 (1982).

[22] A. C. Kibblewhite, R. N. Denham, and D. J. Barnes, ''Unusual low-frequency signals observed in New Zealand waters,'' J. Acoust. Soc. Am. **41**, 644–655 (1967).

[23] D. K. Mellinger and C. W. Clark, ''Characteristics of fin and blue whale vocalizations recorded from IUSS in the north and west Atlantic,'' 11th Biennial Conference on the Biology of Marine Mammals, Orlando, FL, 1995.

[24] J. W. Northrup and W. C. Cummings, ''Underwater 20-Hz signals recorded near Midway Island,'' J. Acoust. Soc. Am. **49**, 1909–1910 (1971).

[25] P. O. Thompson and W. A. Friedl, ''A long term study of low frequency sounds from several species of whales off Oahu, Hawaii,'' Cetology **19**, 1–19 (1982).

[26] J. S. Perkins and W. A. Kuperman, ''Environmental signal processing: Three-dimensional matched-field processing with a vertical array,'' J. Acoust. Soc. Am. **87**, 1553–1556 (1990).
[27] N. O. Booth, P. A. Baxley, J. A. Rice, P. W. Schey, W. S. Hodgkiss, G. L. D'Spain, and J. J. Murray, ''Source localization with broad-band matched-field processing in shallow water,'' IEEE J. Ocean Eng. **21**, 402–412 (1996).
[28] M. D. Collins and W. A. Kuperman, ''Focalization: Environmental focusing and source localization,'' J. Acoust. Soc. Am. **90**, 1410–1422 (1991).
[29] D. F. Gingras and P. Gerstoft, ''Inversion for geometric and geoacoustic parameters in shallow water: Experimental results,'' J. Acoust. Soc. Am. **97**, 3589–3598 (1995).
[30] S. E. Dosso, M. L. Yeremy, J. M. Ozard, and N. R. Chapman, ''Estimation of ocean bottom properties by matched-field inversion of acoustic field data,'' IEEE J. Ocean Eng. **18**, 232–239 (1993).
[31] P. Gerstoft, ''Inversion of seismoacoustic data using genetic algorithms and a posteriori probability distributions,'' J. Acoust. Soc. Am. **95**, 770–782 (1994).
[32] P. Gerstoft, ''Inversion of acoustic data using a combination of genetic algorithms and the Gauss-Newton approach,'' J. Acoust. Soc. Am. **97**, 2181–2190 (1995).
[33] P. Gerstoft and D. F. Gingras, ''Parameter estimation using multifrequency range-dependent acoustic data in shallow water,'' J. Acoust. Soc. Am. **99**, 2839–2851 (1996).
[34] P. Gerstoft, ''SAGA Users Guide 2.0, an inversion software package,'' SACLANT Undersea Research Centre SM-333 (1997).
[35] E. D. Bronson and L. R. Glosten, ''FLIP; Floating Instrument Platform,'' Marine Physical Laboratory, SIO, MPL Tech. Memo MPL-U-27/85 (1985).
[36] ''http://www.nos.noaa.gov/ocrm/nmsp/nmschannelislands.html,'' Vol. 1996, NOAA, 1999.
[37] K. F. Mangels and P. Fiedler, ''Cruise announcement: Whale habitat and prey study (WHAPS95), a marine mammal habitat survey off southern California,'' U. S. Dept. of Commerce, Nat'l Oceanic and Atmos. Admin., Nat'l Marine Fish. Service, Southwest Fish. Sci. Center, Feb (1995).
[38] P. C. Fiedler, S. Reilly, R. P. Hewitt, D. Demer, V. A. Philbrick, S. Smith, W. Armstrong, D. A. Croll, B. R. Tershey, and B. R. Mate, ''Blue whale habitat and prey in the Channel Islands,'' Deep-Sea Res. II **45**, 1781–1801 (1998).
[39] W. S. Hodgkiss, J. C. Nickles, G. L. Edmonds, R. A. Harriss, and G. L. D'Spain, ''A large dynamic range vertical array of acoustic sensors,'' *Full Field Inversion Methods in Ocean and Seismic Acoustics*, edited by O. Diachok (Kluwer, Dordrecht, The Netherlands, 1995).
[40] G. L. D'Spain and W. S. Hodgkiss, ''Array processing with acoustic measurements at a single point in the ocean,'' J. Acoust. Soc. Am. **91**, 2364 (A) (1992).
[41] G. L. D'Spain, W. S. Hodgkiss, and G. L. Edmonds, ''Energetics of the deep ocean's infrasonic sound field,'' J. Acoust. Soc. Am. **89**, 1134–1158 (1991).
[42] L. Davis, *Genetic Algorithms and Simulated Annealing* (Pitman, London, 1987).
[43] D. E. Goldberg, *Genetic Algorithms in Search, Optimization, and Machine Learning* (Addison-Wesley, Reading, MA, 1989).
[44] M. B. Porter, ''The KRAKEN normal mode program,'' SACLANTCEN, Memorandum SM-245, 1991.
[45] J.-M. Q. D. Tran and W. S. Hodgkiss, ''Sound-speed profile inversion using a large aperture vertical line array,'' J. Acoust. Soc. Am. **93**, 803–812 (1993).
[46] P. O. Thompson, ''20-Hz pulses and other vocalizations of fin whales, *Balaenoptera physalus*, in the Gulf of California, Mexico,'' J. Acoust. Soc. Am. **92**, 3051–3057 (1992).
[47] W. A. Watkins, ''Activities and underwater sounds of fin whales,'' Sci. Rep. Whal. Res. Inst. **33**, 83–117 (1981).
[48] W. A. Watkins, P. Tyack, K. E. Moore, and J. E. Bird, ''The 20-Hz signals of finback whales (*Balaenoptera physalus*),'' J. Acoust. Soc. Am. **82**, 1901–1912 (1987).
[49] W. J. Richardson, C. R. Greene, C. I. Malme, and D. H. Thomson, *Marine Mammals and Noise* (Academic, San Diego, 1995).
[50] J. Northrop, W. Cummings, and P. Thompson, ''20-Hz signals observed in the central Pacific,'' J. Acoust. Soc. Am. **43**, 383–384 (1968).
[51] H. Cox, R. M. Zeskind, and M. M. Owen, ''Robust adaptive beamforming,'' IEEE Trans. Acoust., Speech, Signal Process. **35**, 1365–1375 (1987).
[52] R. A. Gramann, ''ABF algorithms implemented at ARL:UT,'' Applied Research Laboratories, University of Texas, ARL-TL-EV-92-31 (1992).
[53] P. K. Yochem and S. Leatherwood, ''Blue Whale,'' in *Handbook of Marine Mammals*, edited by S. H. Ridgway and S. R. Harrison (Harcourt Brace Jovanovich, San Diego, 1985), Vol. 3, p. 223.
[54] G. L. D'Spain, J. J. Murray, W. S. Hodgkiss, N. O. Booth, and P. W. Schey, ''Mirages in shallow water matched field processing,'' J. Acoust. Soc. Am. **105**, 3245–3265 (1999).
[55] W. Perryman, personal communication, 1996.
[56] M. D. Collins, R. J. Cederberg, D. B. King, and S. A. Chin-Bing, ''Comparison of algorithms for solving parabolic wave equations,'' J. Acoust. Soc. Am. **100**, 178–82 (1996).
[57] W. A. Kuperman, M. B. Porter, and J. S. Perkins, ''Rapid computation of acoustic fields in three-dimensional ocean environments,'' J. Acoust. Soc. Am. **89**, 125–33 (1991).
[58] E. L. Hamilton, ''Geoacoustic modeling of the sea floor,'' J. Acoust. Soc. Am. **68**, 1313–1339 (1980).
[59] D. Gorsline, unpublished station data, 1997.
[60] R. T. Bachman, ''Estimating velocity ratio in marine sediment,'' J. Acoust. Soc. Am. **86**, 2029–2031 (1989).
[61] T. C. Yang, ''Broadband source localization and signature estimation,'' J. Acoust. Soc. Am. **93**, 1797–1806 (1993).
[62] S. D. Chuprov, ''Interference structure of a sound field in a layered ocean,'' in *Akustika Okeana. Sovremennoe sostoyanie* (*Ocean Acoustics, Current State*), edited by L. M. Brekhovskikh and I. B. Andreevoi (Nauka, Moscow, 1982), pp. 71–91.
[63] F. B. Jensen and W. A. Kuperman, ''Optimum frequency of propagation in shallow water environments,'' J. Acoust. Soc. Am. **73**, 813–819 (1983).
[64] M. A. McDonald, J. A. Hildebrand, and S. C. Webb, ''On the sound production mechanism of blue whales'' (unpublished).
[65] N. H. Fletcher, *The Physical of Musical Instruments* (Springer-Verlag, New York, 1991).
[66] M. Hendershott, personal communication, 1999.
[67] J. Barlow, personal communication, 1999.
[68] J. Pineada, ''Circulation and larval distribution in internal tidal bore warm fronts,'' Limnology and Oceanography **44**, 1400–1414 (1999).